

*Refereed Proceedings*

*The 13th International Conference on*

*Fluidization - New Paradigm in Fluidization*

*Engineering*

---

Engineering Conferences International

Year 2010

---

RADIAL DISTRIBUTION OF  
PARTICLE CLUSTERS IN A  
DOWNER REACTOR UNIT

Mohammad Ashraful Islam\*

Stefan Krol<sup>†</sup>

Hugo Ignacio de Lasa<sup>‡</sup>

\*The University of Western Ontario

<sup>†</sup>The University of Western Ontario

<sup>‡</sup>The University of Western Ontario, [hdelasa@eng.uwo.ca](mailto:hdelasa@eng.uwo.ca)

This paper is posted at ECI Digital Archives.

[http://dc.engconfintl.org/fluidization\\_xiii/56](http://dc.engconfintl.org/fluidization_xiii/56)

## RADIAL DISTRIBUTION OF PARTICLE CLUSTERS IN A DOWNER REACTOR UNIT

Mohammad Ashraful Islam, Stefan Krol, Hugo I. de Lasa

*Chemical Reactor Engineering Centre, Chemical and Biochemical Engineering  
Department, Faculty of Engineering, University of Western Ontario, N6A 5B9  
London, Ontario, CANADA [hdelasa@eng.uwo.ca](mailto:hdelasa@eng.uwo.ca)*

### ABSTRACT

This study investigates the formation of clusters at 11 radial positions in a 2.63 cm ID downer reactor using the CREC-GS-Optiprobos. Cluster properties such as dimensions, drag coefficients and velocity across the downer unit radius are established based on the reported data and a probabilistic based model.

### INTRODUCTION

In recent years, much interest has been centered on cluster phenomena in downer reactors due to its influence on heat and mass transfer between flowing phases. Researchers at Chemical reactor Engineering Centre, University of Western Ontario, (CREC-UWO) [Krol et al. (1)] developed a model of possible cluster formation in downer reactors using different cluster shape configurations. In this model it was suggested and later validated with CREC-GS-Optiprobos [Nova et al. (2)] that the most probable and stable cluster configuration for the particles evolving in a down-flow unit is the one with individual particles moving as string shaped agglomerates. Furthermore in a recent contribution [Islam et al. (3)] from our group the concept of moving strand shape clusters in stabilized flow region at the centreline of downer unit is described with a drag coefficient function of both Reynolds number and the number of equivalent mean diameter particles contained in the agglomerates.

In the literature, it is reported that the gas-solid flow along the radius of downer is much closer to plug flow in the developed zone [Cheng et al. (4), Wu et al. (5), Deng et al. (6)]. However, a comprehensive investigation about the aggregation behavior of the solid phase is essential to understand the disparity in the slip velocities at various radial positions. This study reports the experimental observations of cluster slip velocities and render a phenomenological approach in terms of cluster drag coefficients,  $C_D$ , for 11 equally spaced radial positions in a downer reactor in constant particle velocity zone.

## EXPERIMENTS

The experiments for this study were conducted in a 2.63 cm ID downer unit made of Acrylic pipe. The height of downer reactor is 3.0 meter. A detail description about the experimental unit is provided by Nova et al. (2). The operating conditions considered in this study are presented in Fig. 1. 14 experimental runs were conducted at ambient temperature with a combination of solid mass fluxes and superficial gas velocities in the range of 10 to 91 kg/m<sup>2</sup>s and 1.2 to 2.5 m/s, respectively. The solid hold up reported in Fig. 1 represents solid concentration at downer centreline. The CREC-GS-Optprobes were inserted into the downer column at 1.85 meters below the air injection port considering that most of the particles will reach at terminal settling velocity at this location. For the reported experimental conditions, the change of pressure gradient along downer height in Fig. 2 shows that below 1.6 meters from the injector the particles/clusters attain fully developed flow pattern (clusters evolving at terminal velocity).

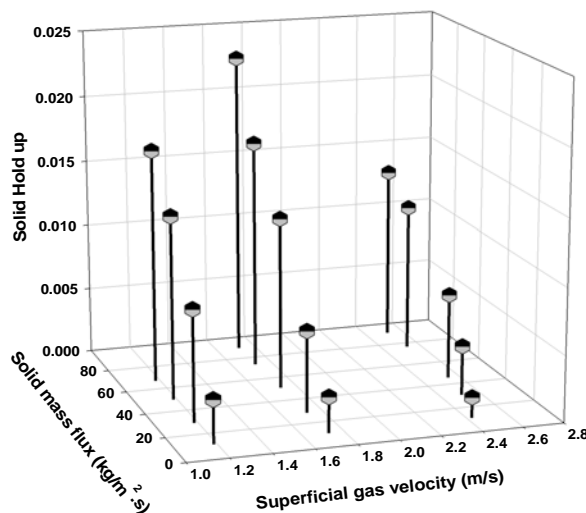


Figure 1: Operating conditions selected for the present study.

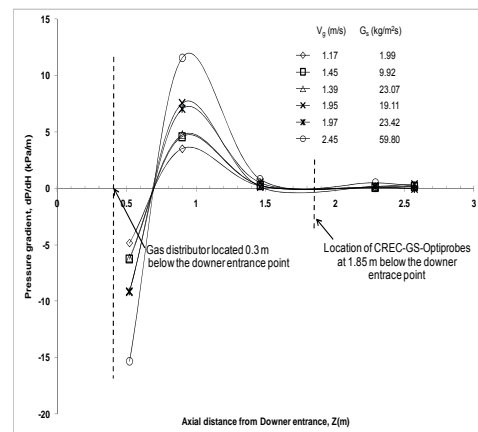


Figure 2: Changes of pressure drop gradients ( $dP/dz$ ) along the downer axial positions. [Islam et al. (3)].

The CREC-GS-Optprobes consists of two probes axially spaced along the flow stream in the downer section. The design principles and calibration procedures of this system are described in Nova et al. (7). For a single operating condition five consecutive signals were collected at 100 kHz. The time delay between two probes, corresponding to the maximum value of the cross-correlation function can be used to estimate the cluster velocity. The evaluation of the cluster size can be based on measurements of the widths of the signal peaks. For each signal an average ( $\bar{X}$ ) and a standard deviation ( $\sigma_x$ ) is calculated. A baseline at average plus three times the standard deviation ( $\bar{X} + 3\sigma_x$ ) is set to eliminate the likely uncorrelated optic signals from the main signal. Fig. 3 can be used to illustrate the evaluation procedure. Further details about data acquisition and data processing are given by Islam et al. (3).

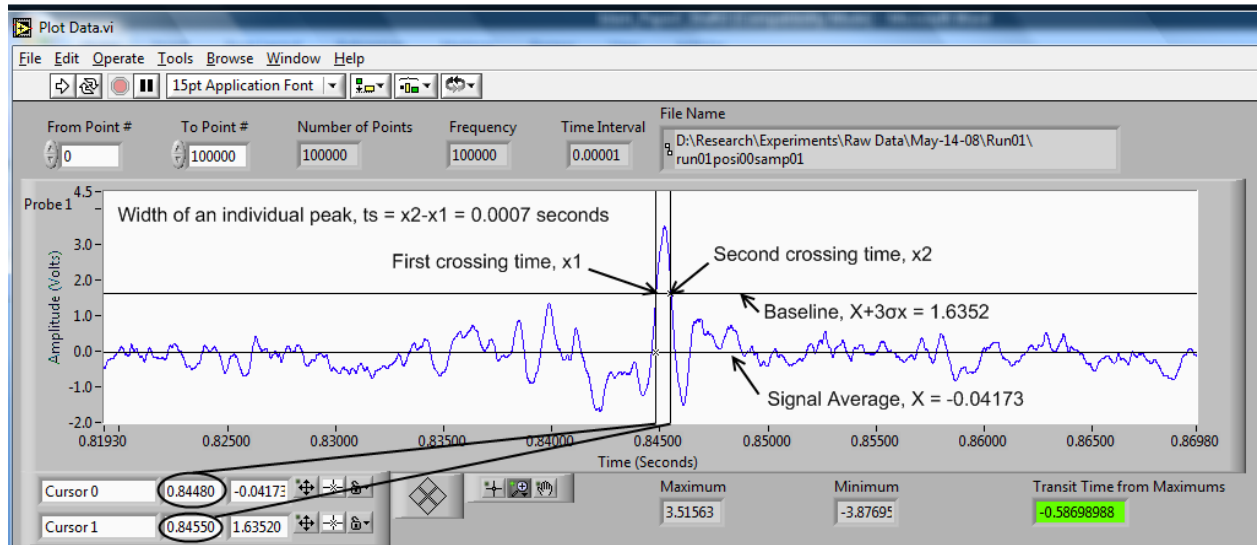


Figure 3: Example of signal peak width determination from the CREC-GS-Optiprobe signals using the  $X+3\sigma_x$  baseline definition. Peaks selected under this criterion differentiate clearly from the signal noise. [Islam et al. (3)]

## DYNAMIC MODELLING OF CLUSTERS

Five pairs of highly correlated signals acquired by CREC-GS-Optiprobe for each operating condition were used to calculate the number of equivalent mean diameter particles ( $N$ ) according to the following equation,

$$N = \frac{t_{s-avg} V_{cl} - h + d_{p,vol-avg}}{d_{p,vol-avg}} \quad (1)$$

with  $t_{s-avg}$  being the average detection time,  $V_{cl}$  the cluster velocity at corresponding pair of time series,  $h$  the characteristic transversal dimension of the sensing region [Islam et al. (8)] and  $d_{p,vol-avg}$  the volume averaged particle size.

According to the cluster configuration proposed by Krol et al. (1) a cluster is likely formed in a downer reactor with a single leading particle and several trailing particles moving in a downward direction. This particle arrangement is the likely one to be found for a fluid dynamically stable cluster. Thus, for the perspective of the present study, the cluster shape can be assumed as a vertical chain of  $N$  number of spherical particles touching each other at their contact points. For this chain like configuration, it is important to consider the actual projected frontal area of the leading particle rather than an area calculated from a volume equivalent diameter of the particles. As well and instead of defining the Reynolds' number based on the diameter of a sphere which has the same volume as the agglomerate, the area weighted average particle diameter from particle size distribution of FCC particles,  $d_{p,area-avg}$ , is used in these experiments as follows:

$$Re = \frac{d_{p,area-avg} V_{slip} \rho_g}{\mu} \quad (2)$$

Where  $V_{slip}$  is the slip velocity,  $\rho_g$  and  $\mu$  are the density and dynamic viscosity of gas respectively.

To characterize the motion of clusters in downer reactors, a possible fundamental approach would be to consider the balance of forces exerted on the dynamic clusters. It is in this respect generally recognized that an accurate and reliable agglomerate drag coefficient,  $C_D$ , could predict the actual behavior of the clusters. In this study, the cluster drag coefficient is defined as a function of both the particle Reynolds' number (Re) and the number of average sized particles (N) contained in the agglomerates. Thus:

$$C_D = \frac{4Ngd_{p,vol-avg}^3(\rho_p - \rho_g)}{3\rho_g d_{p,area-avg}^2 V_{slip}^2} \quad (3)$$

Where,  $d_{p,vol-avg}$  is the volume weighted mean particle diameter,  $d_{p,area-avg}$  is the area weighted average particle diameter,  $V_{slip}$  is the slip velocity,  $g$  is the gravitational acceleration,  $\rho_g$  and  $\rho_p$  are the densities of gas and particle respectively.

## ANALYSIS OF EXPERIMENTAL RESULTS

CREC-GS-OptiprobeS were used to acquire highly cross-correlated signals from 14 experimental runs. Figs 4 and 5 report the radial profiles of solid concentration as well as slip velocities for these runs. For more clear data description only results for 9 operating conditions are reported in these figures. However, the results from the entire set of 14 experimental runs are covered in Fig. 6 & Fig. 7.

Fig. 4 shows essentially flat solid concentration profiles. This agrees very well with the results reported in the literature [Cheng et al. (4), Wu et al. (5), Deng et al. (6)]. In this study it is found that the radial slip velocity profiles at low gas velocities (<2 m/s) display a progressive increase from the column centre to the  $r/R=0.5$  radial position, fluctuating around an average value towards the wall. A distinct behaviour is however observed at gas velocities higher than 2 m/s with maximum slip velocities at the unit centreline with these values decreasing after the radial location at  $r/R=0.5$ . On the other hand Fig. 5 shows that the slip velocities are more sensitive to the change of superficial gas velocities rather than to the solid mass fluxes.

On the basis of a flow description based on a fully developed flow, a drag coefficient function of the Reynolds number and the number of equivalent mean diameter particles in the aggregate, was recently considered [Islam et al. (3)]. Given equations (1) and (3),  $C_D$ , can be calculated for various cluster sizes based on a Reynolds' number (Re) involving the number of equivalent mean diameter particles in every aggregate (N). As it can be seen in Fig. 6, this approach can be extended for various radial positions, with a good correlation (Coefficient of correlation  $R^2 > 0.90$ ) observed between these two parameters.

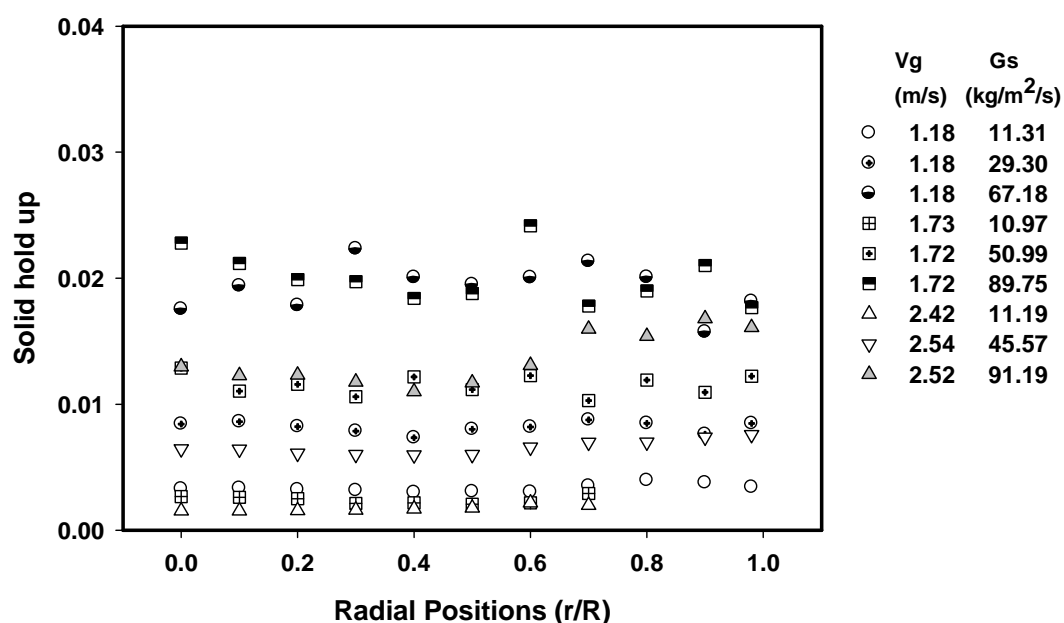


Figure 4: Radial distribution of solid hold up profiles at various solid fluxes (Gs) and superficial gas velocities. Note: Points reported are averages of 5 measurements for each operating condition.

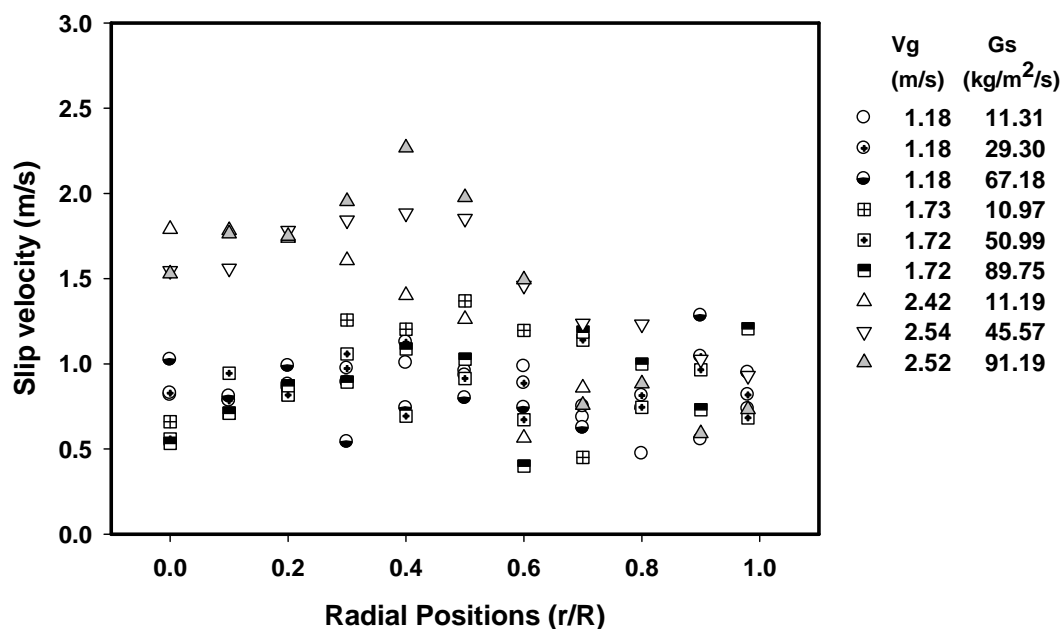


Figure 5: Radial distribution of slip velocity profile at various solid fluxes (Gs) and superficial gas velocities. Note: Points reported are averages of 5 measurements for each operating condition.

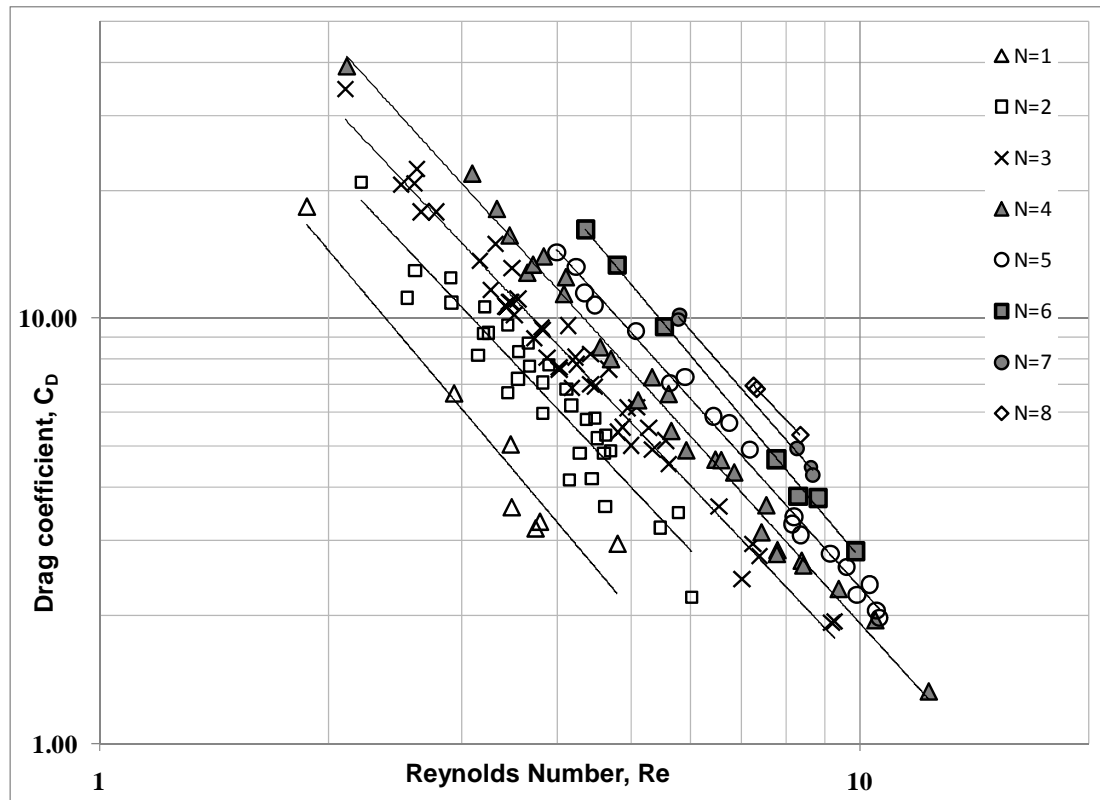


Figure 6: Drag coefficients,  $C_D$ , measured at various radial positions and cluster sizes ( $N$ ). Notes: a)  $\Delta$  for  $N=1\pm0.5$ ,  $\square$  for  $N=2\pm0.5$ ,  $\times$  for  $N=3\pm0.5$ ,  $\blacktriangle$  for  $N=4\pm0.5$ ,  $\circ$  for  $N=5\pm0.5$ ,  $\blacksquare$  for  $N=6\pm0.5$ ,  $\bullet$  for  $N=7\pm0.5$ ,  $\diamond$  for  $N=8\pm0.5$ . b) There is a tight correlation of  $C_D$  with  $Re$  and  $N$  with no observable influence of the radial position.

Furthermore, it is also shown in this contribution that the slip velocity and the axial cluster length or  $N$  can be loosely correlated in down flow reactors. This loose-fitting is the result of the intrinsic nature of the observable particle strands, which involve a diversity of leading and trailing particles of various sizes.

These results can also be validated using a conditional probabilistic simulation where clusters are formed using the Matlab random number generator (RandomMat) [Islam et al. (3)]. Typically a pool of 1000 particles is used with the 1000 particles ensemble showing a frequency particle size distribution as in the FCC particle sample.

The implemented cluster formation simulation randomly picks particles, one by one, and checks the combined total cluster length. If the simulated cluster length is within 1% of the CREC-GS-Optiprobe detected cluster length, this cluster is considered for further computations. The first particle of this selected cluster is labelled the "leading" particle. Its Reynolds number, as well as its projected area and drag coefficient, is accounted in the ensuing evaluation of cluster slip velocity.

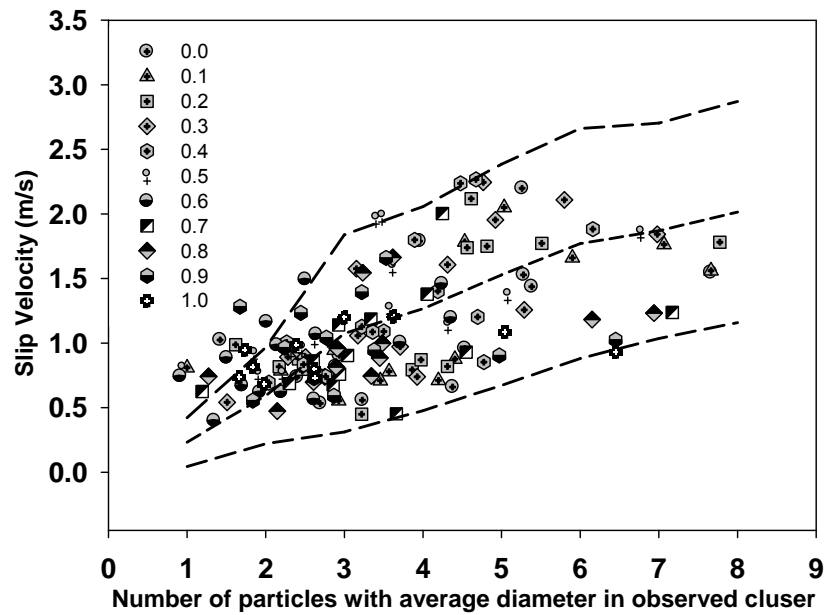


Figure 7: Cluster slip velocities as a function of the number of particles in a cluster. Note: various symbols represent different radial positions. Broken lines reports lowest and highest values of  $V_{slip}$  for a given  $N$ .

Fig. 7, reports  $V_{slip}$  and  $N$  based on the probabilistic based calculations. This yields “lowest” and “highest” slip velocities for a given cluster size and to the definition of a “region” of  $V_{slip}$  and  $N$  correlation (refer to the broken lines in Fig.7).

## CONCLUSIONS

The following are the conclusions of the present study:

- Slip velocities do not vary significantly at various radial positions for a single operating condition. At low gas velocities (<2 m/s), slip velocities increase from the column centre to  $r/R=0.5$ . However, at gas velocities more than 2 m/s a flat slip velocity profile decreases after this radial location ( $r/R=0.5$ ).
- Cluster slip velocities are primarily influenced by the gas velocities rather than solid mass fluxes and/or radial position.
- A model is developed to describe the cluster behaviour in a downflow reactor. This probabilistic based model provides a range of cluster velocities encompassing the various possible particle combinations of slip velocities and cluster sizes.

## NOTATION

$C_D$	Drag coefficient
$d_{P,vol-avg}$	Volume weighed mean particle diameter (m)



$d_{P,area-avg}$	Area weighted mean particle diameter (m)
$G_s$	Solid mass flux (kg/m <sup>2</sup> s)
$g$	Gravity acceleration (m/s <sup>2</sup> )
$h$	Characteristic transversal dimension of the sensing region (focal point) (m)
$N$	Number of particles in a cluster with diameter $d_{P,vol-avg}$
$Re$	Reynolds number based on area weighted mean particle diameter,
$V_g$	Superficial gas velocity (m/s)
$V_{cl}$	Cluster velocity (m/s)
$V_{slip}$	Slip velocity (m/s)
$X$	Signal average (volt)
$t_{s-avg}$	Average of peak width (second)
$\mu$	Gas kinematic viscosity (kg/m/s)
$\rho_g$	Density of the gas (kg/m <sup>3</sup> )
$\rho_p$	Density of the particle (kg/m <sup>3</sup> )
$\sigma_X$	Standard deviation of signal (volt)

## REFERENCES

1. Krol, S., Pekediz, A., de Lasa, H. I., Powder Technology, 2000, 108, 6-20.
2. Nova, S. R., Krol, S., Lasa, H. I., Powder Technology, 2004, 148, 172-185.
3. Islam, M. A., Krol, S., de Lasa, H. I., Accepted in Industrial and Engineering Chemistry Research.
4. Cheng, Y., Wu, C., Zhu, J., Wei, F., Jin, Y., Powder Technology, 2008, 183, 364-384.
5. Wu, B., Zhu, J. -X., Briens, L., Zhang, H., Powder Technology, 2007, 178, 187-193.
6. Deng, R., Wei, F., Liu, T., Jin, Y., Chemical Engineering and Processing, 2002, 41, 259-266.
7. Nova, S. R., Krol, S., Lasa, H. I., Industrial and Engineering Chemistry Research, 2004, 43, 5620-5631.
8. Islam, M. A., Krol, S., De Lasa, H. I., Focal Region Definition Using CREC-GS-Optiprbes. In Preparation.